Optical Interconnection Network for Massively Parallel Processors Using Beam-Steering Vertical Cavity Surface-Emitting Lasers

L. Fan and M. C. Wu

UCLA, Electrical Engineering Department
66-147D Engineering IV, 405 Hilgard Avenue,
Los Angeles, CA 90095-1594

H. C. Lee and P. Grodzinski

Motorola Inc. Phoenix Corporate Research
Laboratories, Tempe, Arizona 85284

Abstract

An ultra-dense optical interconnection network is proposed for massively parallel processors. Using two-dimensional arrays of beam-steering vertical cavity surface-emitting lasers (VCSEL) as space-division switching elements, a single-chip, free-space photonic banyan network (or other multi-stage networks) can be constructed. Our scheme does not require critical optical alignment and can be easily packaged in compact chips. The optical beam steering of VCSELs are realized with an integrated beam router. Steering angles as large as 10° from surface-normal direction has been demonstrated. The VCSEL has a threshold current of 4 mA and output power of 1 mW (for 4μm×8μm device) and a modulation bandwidth of 10 GHz. Dynamic switching of optical beam angles at 2 GHz has been demonstrated.

1. Introduction

Massively parallel computer systems with a large number of processors could significantly improve the speed of high-performance computers. Since communications overhead is one of the most important factors affecting the performance of parallel processors, there has been a great deal of research interest in their interconnection networks. Various types of networks including hypercube, mesh, and various type of multi-stage interconnection networks have been implemented.

Optics is ideally suited for implementing these interconnection networks because of its inherent parallelism, high speed (> 10 Gbps), high spatial bandwidth, low signal crosstalk, and capability of wavelength-division multiplexing through a common media [1]. Early demonstration of optical interconnect in massively parallel processors (MPP), such as Intel's Touchstone [2] and Thinking Machine's Connection Machine [3], employs optical fibers and exploit the speed advantages of fiber links. Such optical interconnect is a direct extension of point-to-point optical communication systems. Recently, there has been a great deal of interest to use free-space optics to implement much denser interconnection networks [4], particularly for MPP applications. For example, a six-stage banyan interconnection has been realized using computer generated holograms and self-electro-optic-effect device (SEED) arrays [5]. An optical hypercube [6] and an optical multi-mesh hypercube [7] have also been proposed using free-space optics and holograms.

On the optoelectronic device side, devices with surface-normal optical access are usually preferred because of their capability to form two-dimensional arrays. Two types of devices are usually employed: modulators such as SEEDs [4,5] and optical emitters such as vertical cavity surface-emitting lasers (VCSEL) [8]. The VCSEL approach has the advantage that no external light source is needed to power the optical system and more compact system may be constructed. Recently, VCSELs with threshold currents below 100 μA have been demonstrated [9]. Thus extremely low-power interconnection (a very important consideration for MPPs) systems can be constructed.

There are two basic components in generic free-space optical interconnect: optoelectronic device for photon generation or modulation; and optical beam routers to redirect or distribute optical beams [1]. Even though the optoelectronic devices including VCSELs and SEEDs can usually be integrated in very compact two-dimensional arrays, the overall system volume is dominated by optical elements for beam routing. Optical beam routing in free-space optical interconnect often employs external optics such as prisms, lenses, gratings or computer generated holograms. These components occupy significant space which limit the density of optical interconnect, and they are not suitable for wafer-

0-8186-7101-7/95 $4.00

scale integration. It is therefore desirable to integrate the beam steering function with the VCSEL source.

In this paper, we present a novel *photonic banyan interconnection chip* employing VCSELs with integrated optical beam steering function. This highly integrated chip requires only an external mirror to fold the optical beams back to the chip. No critical optical alignment is needed. The optical beam steering is achieved by adding a non-perturbing optical phase shifter on part of the VCSEL surface [10]. A non-perturbing phase shifter does not change the reflectivity of the VCSEL and which is necessary to preserve the fundamental spatial mode operation of the VCSEL. By removing or adding a layer of material with thickness equal to an integral multiple of half wavelength to the surface of the VCSEL, the emitted light from the VCSEL passing through the phase-shifter experiences an additional phase shift of $\pi \cdot (n-1)/n$, where n is the refractive index of the phase-shifter. We have fabricated a beam-steering VCSEL with half of the VCSEL area covered by a GaAs phase-shifter. Beam steering angles from 2° to 10° have been observed, in good agreement with the theory. Dynamic switching with electric injection can also be easily implemented. The switching speed is of the order of the relaxation oscillation frequency. Dynamic switching between the 0° and 3° optical beams at 2 GHz has been experimentally demonstrated. In each emission, the data can be modulated up to the 3 dB bandwidth of 10 GHz. This unique design preserves all the advantages of VCSEL's, including low threshold currents, narrow beam diverging and the ability to form tow dimensional arrays, while adding the new capability of beam steering. Two-dimensional optical beam steering can also be implemented.

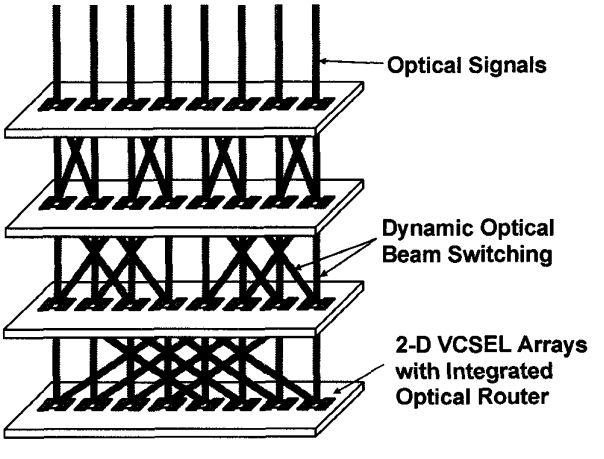

Fig.1. Schematic diagram of a photonic banyan network constructed with beam steering VCSELs.

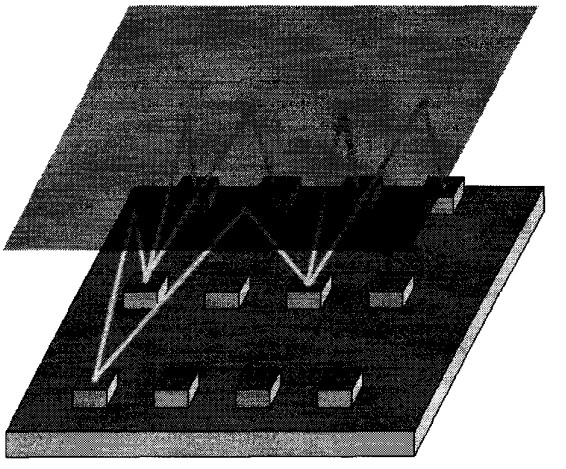

Fig. 2. A folded cavity enabling the photonic banyan network to be integrated on a single chip with two-dimensional arrays of beam-steering VCSELs.

2. Fundamental Principle

By employing VCSELs with integrated beam routers, a multi-stage banyan network can be realized by simply cascading several planes of VCSEL arrays, as illustrated in Fig. 1. Each switching node consists of a VCSEL and an optical beam router. By controlling the emission direction, 2 x 2 optical switches can be realized in free-space. The beam switching angles can be varied in different stages, thus very compact interconnection network can be constructed using cascaded stages of such switching nodes. However, this implementation requires several planes of switching nodes which prevent the system to be integrated on a single chip. By using a folded optical cavity in which optical beams bouncing back and forth in a zigzag way, all the optoelectronic switching nodes can be arranged in a two-dimensional array. This is illustrated in Fig. 3. Unlike planar optics approach [11,12], only a planar mirror is needed for external optics in this approach, therefore, optical alignment tolerance is much more relaxed.

By integrating the optical beam routers with light sources, the volume of the switching node can be greatly reduced. The principle is illustrated in Fig. 3. Vertical cavity surface-emitting lasers (VCSEL) are used here as optical sources because they have many advantages such as low threshold currents, low beam divergence, and the ease to form two-dimensional arrays. Ideally, a prism can be integrated on top of a VCSEL to steer the output beam. However, a continuous tone prism is difficult to produce with standard microfabrication techniques. Instead, a step-wise prism is incorporated on top of the VCSEL.

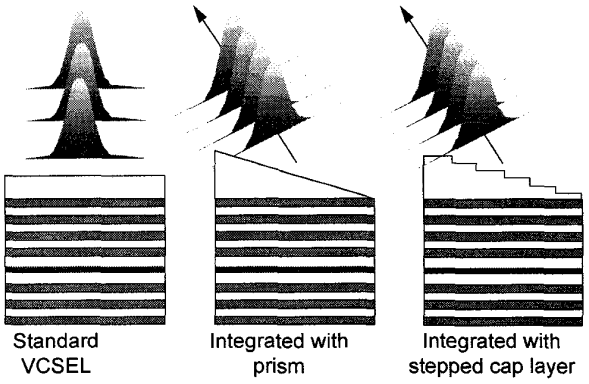

Fig. 3. Principle of the monolithically integrated optical beam router on VCSELs for massively parallel computers.

We have implemented a two-step prism as optical beam router by etching the top semiconductor layer of the VCSEL structure. In forming the prism, it is very important that the prism does not interfere with VCSEL operation. For example, the optical beam router should not increase the threshold current of the VCSEL, and more importantly, does not introduce high-order spatial modes. However, it is known that the reflectivity of the VCSEL is a very sensitive function of the terminating phase of the distributed Bragg reflector (DBR) cap layer. In fact, the reflectivity drops dramatically when the etched layer thickness is equal to a quarter wavelength. On the other hand, if the etched layer thickness is equal to half wavelength, both the amplitude and phase of the reflectivity is virtually unchanged. Therefore, if we keep all the prism step thickness to integral multiples of half wavelength, the VCSEL cavity is least disturbed and same threshold current and fundamental mode operation can be maintained.

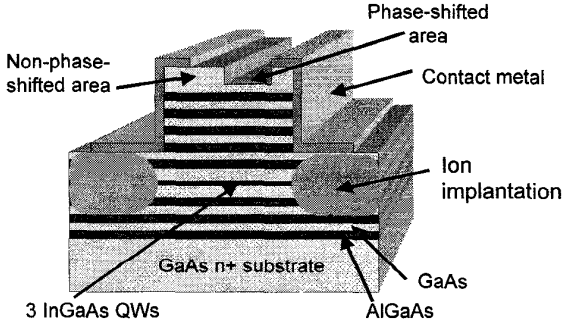

Fig. 4. The schematic diagram of the VCSEL with an integrated optical beam router.

Phase correctors have been used to achieve a single-lobe far-field pattern from a phase-locked two-dimensional VCSEL arrays [13]. A much thicker phase shifters with thickness equal to five times of half wavelengths is employed. A Fresnel zone VCSEL with focusing output beams has also been demonstrated that uses etching to control the transverse mode of the VCSEL [14]. However, both of these approaches rely on large VCSEL areas which result in high threshold currents. Beam steering of edge-emitting laser has been proposed using twin waveguides [15]. The principle is similar to our approach here, however, the use of edge-emitting lasers limits the steering direction to one dimension only. The VCSELs have an additional advantage that the phase shifters can be processed using conventional microfabrication techniques and is suitable for wafer scale integration.

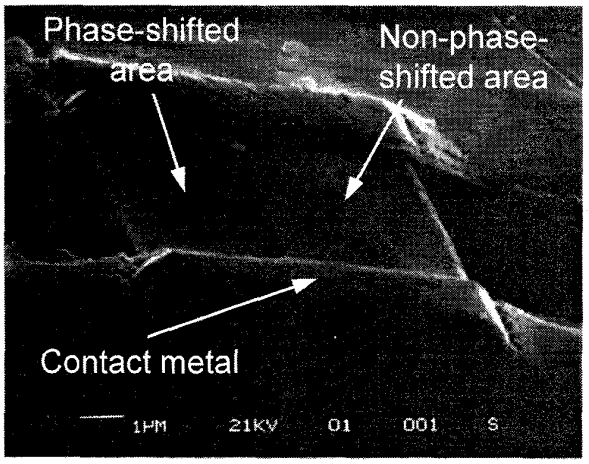

Fig. 5. The SEM photograph of the VCSEL with integrated optical beam router.

The schematic structure of the integrated beam router is illustrated in Fig. 4. A non- perturbing phase-shifter is formed by selectively etching the VCSEL cap layer by 1/2 wavelength. The etched part creates an phase shift of $\frac{2\pi}{\lambda}\cdot(n-1)\cdot\frac{\lambda}{2n}=\left(1-\frac{1}{n}\right)\cdot\pi=129^{\circ}$ for cap layer refractive index n = 3.52. When both the phase-shifted region and the non-phase-shifted region are electrically pumped simultaneously, these two beams interfere and steer the output beam to off surface-normal directions. The devices are fabricated in the Nanofabrication Research Facility at UCLA. The scanning electron micrograph (SEM) of the finished device is shown in Fig. 5. Devices capable of dynamic beam switching are also fabricated, as will be discussed in more detail later.

3. Experimental Results

3.1 Static optical beam switching

The experimental results of static and dynamic optical beam switching operation are described in this section. Figure 6 shows the experimental and the theoretically simulated far-field patterns of a VCSEL with 6μm-wide phase-shifted region and 6μm-wide non-phase-shifted region. The main output beam is steered from 0° to 2.9°, in good agreement with the theoretical prediction. The shape of the far-field pattern also agrees very well with theory.

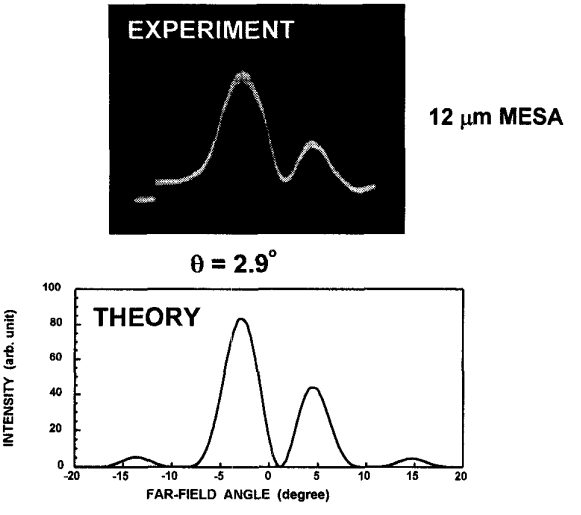

Fig. 6. The experimental and theoretically simulated far-field patterns of the VCSEL with optical beam router. The main beam has been steered by 2.9°

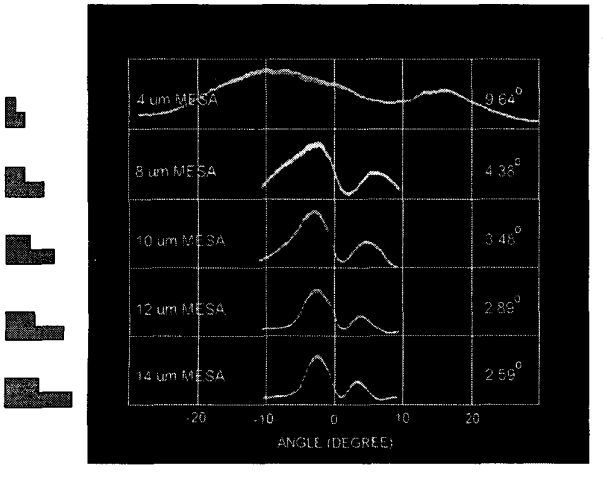

Fig. 7. Experimental far-field patterns of the VCSELs with various optical beam routers. Steering angles as large as 9.6° are achieved.

The steering angle is determined by the center-to-center spacing of the phase-shifted and non-shifted regions and the refractive index of the phase-shifter. Therefore, by properly designing the devices, various steering angles can be achieved. This is illustrated in Fig. 7, beam steering angles from 2.6° to 9.6° are obtained when the center-to-center spacing (which is equal to half of the mesa size in our current design) is varied from 7μm to 2 μm. They also agree very well with the theoretical prediction (Fig. 8). It should be noted that the wider beam width of the VCSELs with larger steering angles results from their smaller total mesa size, as illustrated in the schematic diagrams on the left hand side of Fig. 7. It is, however, not a fundamental limitation of this design. In order to maintain the same beam width, the repetitive steps can be incorporated on the same total mesa area.

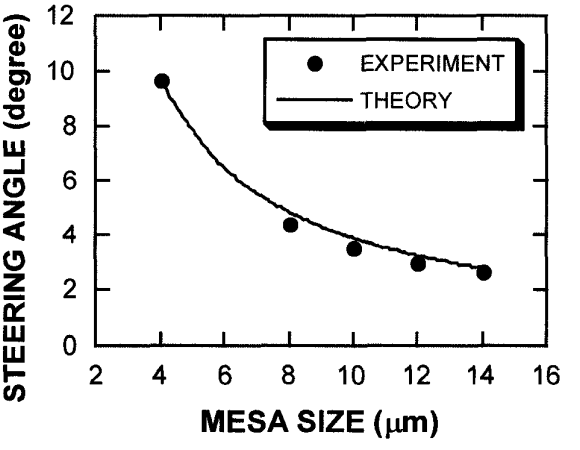

Fig. 8. The optical beam steering angle as a function of the mesa size. The mesa consists of half phase-shifted and half non-phase-shifted regions.

3.2 Dynamic optical beam switching

Dynamic switching of the optical beams is also successfully demonstrated. It is achieved by independently controlling the injection currents in the phase-shifted and non-phase-shifted regions, as illustrated in Fig. 9. when only the non-phase-shifted region (or phase-shifted) is turned on, the device behaves like a standard VCSEL and surface-normal output beams are obtained. On the other hand, when both regions are pumped simultaneously, the optical beam is steered to off surface-normal directions as described earlier. The SEM photograph of the finished device is shown in Fig. 10. The phase-shifted region is realized by etching a half-wavelength-thick layer off the top GaAs layer. Switching of the optical beams is observed by imaging the far-field

pattern onto a CCD camera. The results are shown in Fig. 11.

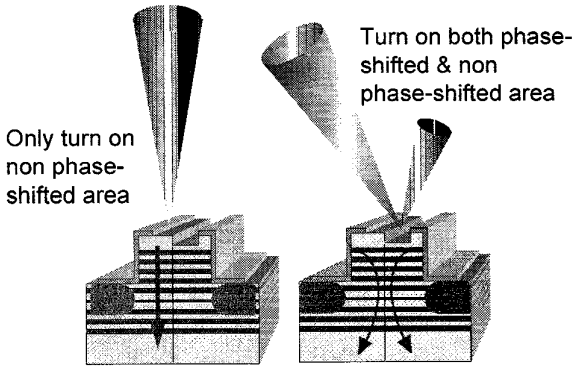

Fig. 9. Dynamic optical beam switching in VCSELs with integrated beam routers.

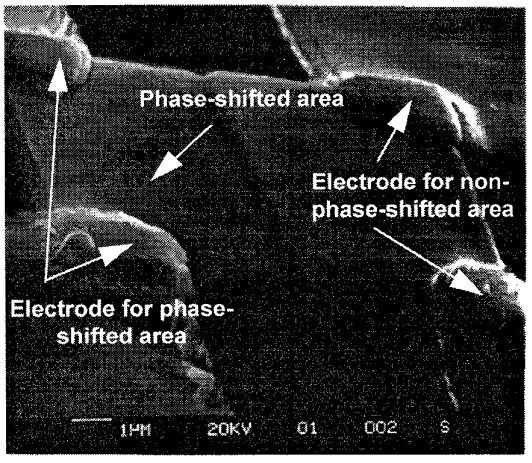

Fig. 10 The SEM photograph of the VCSEL with dynamic optical beam router.

A circular output beam in the surface-normal direction is observed when only the non-phase-shifted region is pumped, as in a standard VCSEL (Fig. 10). When the phase-shifted region is also turned on, the optical beam is switched to 2.9° off the surface-normal direction for this 12μm-wide device. The far-field pattern clearly shows the switching (Fig. 11). The minor lob, resulting from the discrete-step design of the optical beam router, is also visible in the CCD image. The minor lobe can be minimized by properly design the optical beam router. This is one of our research topics in the next Quarter.

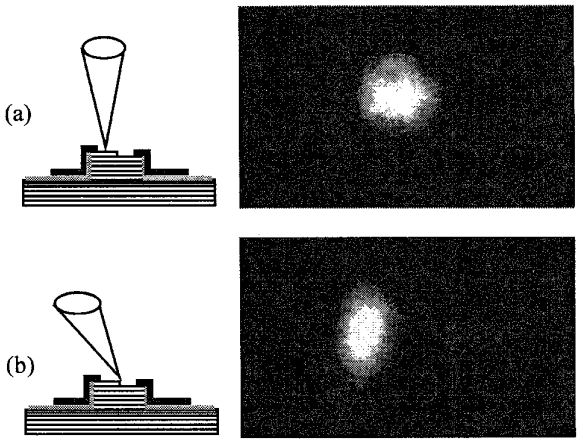

Fig. 11 Far field pattern of the dynamic spatial switching the emitting angle of VCSEL controlled by individually pumping the different mesa areas. (a) only pumped the non-phase-shift area. (b) pumped both phase-shift and non phase-shift areas.

3.3 Switching speed of the dynamic beam router

The switching speed of this dynamic beam-steering device is also investigated experimentally. Even though the switching of the optical beam is used to reconfigure the optical interconnect network and very high speed reconfiguration of the interconnection network is usually not required, it is interesting to find out the ultimate performance of this device. The experimental setup for testing the dynamic switching is shown in Fig. 12.

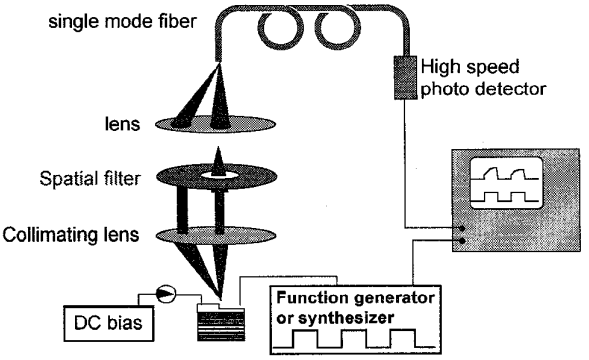

Fig. 12 The experimental setup for measuring dynamic beam switching. The spatial filter can select either the surface-normal beam or the steered beam. The signal is displayed on a sampling scope.

The non-phase-shifted region is kept on a fixed DC bias while the phase-shifted region is modulated by a function generator (square wave up to 10 MHz) or a frequency synthesizer (sine wave up to 26 GHz). The output light from the beam-steering VCSEL is first collimated by an objective lens and then focused into a single mode fiber. The signal is detected by a high speed photodetector and then displayed on a sampling scope. The switched and non-switched beams can be separated by inserting a spatial filter between the two lenses. The results of dynamic switching of the device under a 1 MHz square wave modulation is shown in Fig. 13. The bottom trace is the modulating signal. The top trace is the response of the surface-normal beam (non-switched beam), which is out of phase with the modulating signals. The middle trace is the steered beam signal, which is in phase with the modulating signal. Very clear switching behavior is observed.

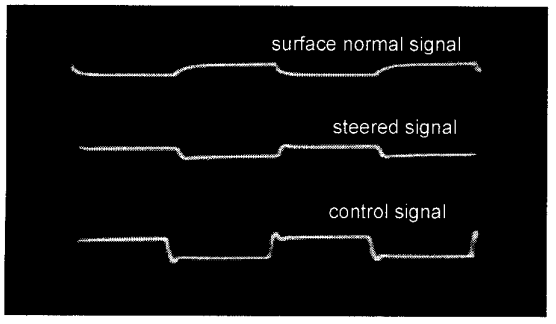

(a) 1 MHz

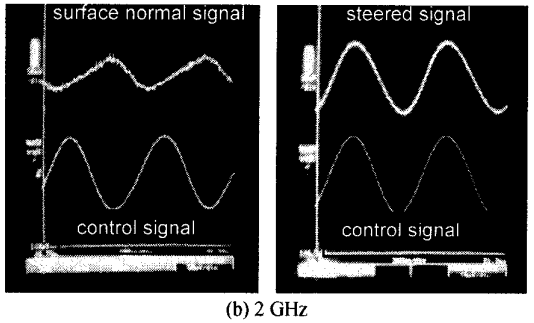

(b) 2 GHz

Fig. 13 Dynamic optical beam switching at a switching rate of (a) 1 MHz, (b)2 GHz. The surface-normal signal is out of phase with the modulating signal (applied to the phase shifted region) while the switched beam is in phase with the modulating signal.

The rising and falling edges of the top trace result from the biasing circuit of the photodetector (1 kΩ resistor is used to boost up the signal voltage), and is not due to the switching response of the device. Switching experiment at 2 GHz is also conducted using a sine wave modulation from a frequency synthesizer. An rf amplifier is employed to enhance the signal. Clear switching is observed at this frequency. Above 2 GHz, the in-phase and out-of-phase signal start to mix together. We believe the switching response can be further improved by optimizing the electric isolation between the phase-shifted and non-phase-shifted regions, and is ultimately limited by relaxation oscillation frequency (~10 GHz in our current device).

3.4 Photonic Banyan interconnection chip

The 4×4 banyan network switch is integrated on a single chip and wire bonded to the package. The emitting signal from the VCSEL is folded back to the photo-detector by an gold coated reflector. The critical rotation angle of the mesa and the steering angle of the beam router are monolithically integrated on a single chip. The height of the reflector is designed to matched the cavity depth of the package. By dropping in the cover lid on top of the package, it is accurate enough to reflect the signal back to the photodetector. By turning on different optical beam routers, the signal is steered to different channels. Figure 14 shows the switching of this photonic banyan interconnection chip. The signal will either stay in the same channel (Fig 14 (a)); or shuffle to other channels (Fig. 14 (b),(c)). This optical banyan inter-connection chip has the advantage of high signal bandwidth transmission of optical system, eliminate the need of critical alignment, and removes the bulky optical components. The chip is sealed in an IC package which can be easily mounted on the circuit board.

Conclusion

A *single-chip photonic banyan interconnection network* based on a novel beam-steering vertical cavity surface-emitting lasers (VCSEL) has been proposed for massively parallel processors. Dynamic optical beam routers have been monolithically integrated with standard VCSEL. Optical beams output from VCSEL are successfully steered by as much as 10° from the surface-normal directions. Dynamic switching of optical beams in space division is also demonstrated up to 2 GHz. This novel device can greatly simplify the architecture of free-space optical interconnect, reduce the volume of optical

interconnect module and hence increase its functional density. The performance of the photonic banyan chip will be discussed in the conference.

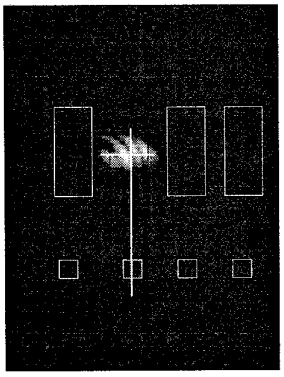

(a) Signal is maintained in the same channel

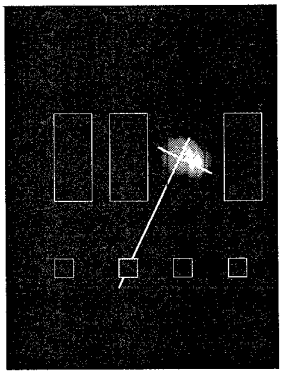

b) Signal is steered to the adjacent channel

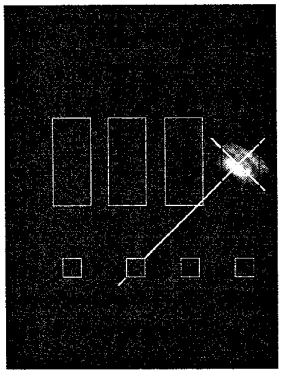

(c) Signal is steered to the next adjacent channel

Fig. 14 Far field pattern from VCSEL is steered by the optical beam router and is recorded on the CCD camera.

Acknowledgment

This project is supported by ARPA ULTRA through Army Research Laboratory under contract No. DAAL01-93-K-3353 and the Packard Foundation.

References

[1] J. W. Goodman, F. J. Leonberger, S. C. Kung, and R. A. Athale, "Optical interconnection of VLSI systems," Proc. IEEE, Vol. 72, p. 850, 1984.

[2] B. E. Floren, T. A. Lane, D. S. Dunning, J. D. Kessinger, S. F. Nugent, and R. L. Traylor, "Optical interconnects in the Touchstone supercomputer program," Proc. SPIE, Vol. 1582, p. 46, 1991.

[3] B. O. Kahle, E. C. Parish, T. A. Lane, and J. A. Quam, "Optical interconnets for interprocessor communications in the Connection Machine," IEEE Conference on Computer Design, Oct. 1989.

[4] H. S. Hinton, et al., "Free-Space Digital Optical Systems," Proc. IEEE, Vol. 82, p. 1632, 1994.

[5] F. B. McCormick, et al., "A six-stage digital free-space optical switching networks using S-SEEDs," Applied Optics, Vol. 32, p. 5153, 1993.

[6] L. A. Bergman, W. H. Wu, A. R. Johnston, R. Nixon, 5. C. Esener, C. C. Guest, P. Yu, T. J. Drabik, M. Feldman, and S. H. Lee, "Holographic optical interconnects for VLSI," Opt. Engin., Vol. 25, p. 1109, 1986.

[7] A. Louri and H. Sung, "An optical multi-mesh hypercube: a scalable optical interconnection network for massively parallel computing," J. Lightwave Technol., Vol. 12, p. 704, 1994.

[8] See for example, J. L. Jewell, J. P. Harbison, A. Scherer, Y. H. Lee, and L. T. Florez, "Vertical-cavity surface-emitting lasers: design, growth, fabrication, characterization," IEEE J. Quantum Electron., Vol. 27, p. 1332, 1991, and the references therein.

[9] D. L. Huffaker, J. Shin, and D. G. Deppe, "Low threshold half-wave vertical-cavity lasers," Electronics Letters., Vol. 30, p. 1946, 1994.

[10] L. Fan, M. C. Wu, H. C. Lee, and P. Grodzinski, "Novel Vertical-Cavity Surface-Emitting Lasers with Integrated Optical Beam Router for Massively Parallel Free-Space Interconnection," 1994 International Electron Device Meeting (IEDM), San Francisco, California, December 11-14, 1994.

[11] J. Jahns, and B. Acklin, "Planar optics: a system technology for integrated optoelectronics," in Diffractive and Miniaturized Optics, edited by Sing H. Lee (SPIE Press, 1994).

[12] S. H. Lee, V. H. Ozguz, J. Fan, D. Zaleta, and C. K. Cheng "Computer aided design and packaging optoelectronic systems with free space optical interconnects," Proceeding of IEEE Custom Integrated Circuits Conference, p. 29.3.1-29.3.4, 1993

[13] M. E. Warren, P. L. Gourley, G. R. Hadley, G. A. Wawter, T. M. Brennan, B. E. Hammons, and K. L. Lear, "Ox-axis far-field emission from 2-dimensional phase-locked vertical cavity surface emitting laser arrays with an integrated phase-corrector," Appl. Phys. Lett., Vol. 61, p. 1484, 1992.

[14] D. Vakhshoori, M. Hong, M. Asom, R. E. Leibenguth, J. P. Mannaerts, and J. D. Wynn, "Zone lasers," Appl. Phys. Lett., Vol. 65, p. 144, 1994.

[15] H. Itoh, S. Mukai, M. Mori, M. Watanabe, and H. Yajima, "Binary logic operations using a beam-scanning laser diode," Optical Engineering, Vol. 31, p. 799, 1992.